NAVORD REPORT 3834

FC

STAGNATION TEMPERATURE PROBES FOR USE AT HIGH SUPERSONIC SPEEDS AND ELEVATED TEMPERATURES

12 OCTOBER 1954

U. S. NAVAL ORDNANCE LABORATORY
WHITE OAK, MARYLAND

Aeroballistic Research Report 256

STAGNATION TEMPERATURE PROBES FOR USE AT HIGH SUPERSONIC SPEEDS AND ELEVATED TEMPERATURES

Prepared by:

E. H. Winkler

ABSTRACT: Stagnation temperature probes with single platinum or gold coated shields made of silica (or other material of low thermal conductivity) were built for use at high supersonic speeds and elevated temperatures. For free-stream Reynolds numbers of the order of 40,000 the temperature recovery factor of the probes reaches .998. It decreases with decreasing Reynolds number and increasing temperature. At temperatures up to 800° K the major thermometric losses of the probes are conduction losses. A single calibration curve is obtained for each probe by relating the calibration data to the flow conditions inside the probe. This calibration curve facilitates the evaluation of flow data from measured pressure and temperature data alone without resorting to any assumptions. Small probes of 1 mm height at the air entrance were successfully used for temperature surveys of turbulent boundary layers on the nozzle wall of the hypersonic tunnel.

U. S. NAVAL ORDNANCE LABORATORY
WHITE OAK, MARYLAND

This report presents results of the development of stagnation temperature probes for use at high supersonic speeds and elevated temperatures. This program was initiated in 1951 to obtain a temperature probe suitable for the range of flow conditions encountered in the NOL Hypersonic Tunnel No. 4. The basic design and some results of the performance of the probes were already reported in reference (a). The complete program presented in this report includes investigations of certain modifications in the design to improve the performance of the probes as well as to extend the range in which they can be used.

The program was sponsored jointly by the U. S. Navy, Bureau of Ordnance and the U. S. Air Force. It was carried out under USAF MIPR AEDC-54-1 and Task NOL-M9a-108-1-54.

The author wishes to acknowledge the cooperation of Messrs. W. L. Clark, H. Hoyt, and R. Garren in manufacturing the probes. Mr. R. Garren also participated in the tests.

JOHN T. HAYWARD
Captain, USN
Commander

H. H. KURZWEG, Chief
Aeroballistic Research Department
By direction

CONTENTS

ILLUSTRATIONS

SYMBOLS

c	specific heat
c_p	specific heat at constant pressure
D	wire diameter
h_c	convection heat transfer coefficient
k	thermal conductivity
L	exposed length of thermocouple wire
M	Mach number
Nu	Nusselt number $(h_c D/k)$
p	static pressure
p_o	supply pressure
p_o'	pitot pressure
Pr	Prandtl number $(c_p \mu/k)$
R	gas constant
r	recovery factor
Re	Reynolds number $(\rho uD/\mu)$
T	local temperature
T_o	stagnation temperature
T_e	equilibrium temperature for zero heat transfer
T_i	temperature indicated by probe
u	velocity
x	length
y	distance perpendicular to wall

α	absorptivity
γ	ratio of specific heats
ε	emissivity
μ	absolute viscosity
ρ	density
σ	Stefan-Boltzmann constant
τ	time constant

Subscripts

∞	values based on free stream conditions
2	values based on conditions behind normal shock
3	values based on conditions inside probe
g	physical properties of gas
d	properties and conditions of shield around thermocouple
b	conditions of thermocouple support
w	properties of thermocouple wire
ref	designates a reference value

STAGNATION TEMPERATURE PROBES FOR USE AT HIGH SUPERSONIC SPEEDS AND ELEVATED TEMPERATURES

INTRODUCTION

1. Stagnation temperature probes suited for use at elevated temperatures have been developed for temperature surveys in the NOL 12 x 12 cm Hypersonic Tunnel No. 4.* Usually, temperature probes for use at supersonic speeds and elevated temperatures have two or more vented shields around the sensing thermocouple (reference (c)). These shields serve to direct the flow, maintain known flow conditions around the thermocouple, and minimize the heat loss from the air sample the temperature of which is to be measured. For boundary layer studies in a wind tunnel a small probe, of the order of 1-mm height at the air entrance, is desirable in order to obtain a sufficient number of data points through the boundary layer. Such a small probe is easier to assemble, if built with a single shield around the thermocouple.

2. Material and finish of the shields, length and diameter of the thermocouple wires, as well as vent area and size of the probe, are parameters affecting the temperature recovery of the probe. It was felt that single-shielded probes can be made to perform comparably to multiple-shielded probes by proper selection of these parameters. This would require, in particular, the use of a material of low thermal conductivity for the shield and the thermal insulation of shield and thermocouple support from the probe holder.

3. Some of the probes which will be described were made rather large (6-mm outside diameter) to facilitate their handling during preliminary investigations. These probes are small enough, however, to obtain a number of data points in the rather thick (about 20 mm) nozzle wall boundary layer of the NOL Hypersonic Tunnel (reference (d)). Probes of 1-mm height at the air entrance built during the course of the present investigations were used for detailed surveys of the temperature variations across the nozzle wall boundary layers.

Description of the Probes

4. All the probes investigated follow the same basic design, as shown in Figure 1. The shield is made of silica or other low-conducting material with both surfaces platinum or gold coated to reduce conduction losses through the shield and

*The hypersonic tunnel operates at Mach numbers between 5 and 10 at supply pressures up to 50 atmospheres and supply temperatures up to 800° K (reference (b)).

radiation losses from the shield surface to cooler surroundings. The shield is cemented to the stainless steel holder with a thermally insulating cement*. Two vent holes provide a continuous replacement of the air inside the probe. The thermocouple is 30 or 38 gauge (Brown and Sharpe Gauge) iron-constantan wire. It is Fiberglas insulated and sealed into a silica support with thermally insulating cement. The exposed surface of the support is also platinum or gold coated. The various probes investigated differed as follows:

a. In the ratio of vent-hole area to entrance area

b. In the shield design

c. In the length of the thermocouple projection above its support

Each of the three parameters was varied separately, with the other two kept constant.

5. Each of the probes was tested over a wide range of flow conditions, i.e. Mach numbers, temperatures, and Reynolds numbers. These calibration data are expressed in terms of a temperature recovery factor of the probe and are related to either a free-stream Reynolds number or the flow conditions inside the probe. The temperature recovery factor of the probe is defined as

$$r = \frac{T_i - T_\infty}{T_o - T_\infty} \qquad (1)$$

where the stagnation temperature, T_o, is set equal to the area-weighted average value of the supply air temperature as obtained from a survey in the nozzle entrance duct (reference (f)), and the free stream temperature, T_∞, is calculated from compressible flow tables (reference (g)). The range of Reynolds numbers that could be covered for each Mach number is determined by the operational range of the hypersonic wind tunnel. For each Mach number, the supply temperature selected was high enough to avoid air condensation in the wind tunnel test section; the supply pressure was then varied so that the set temperature could be maintained with the heater power available. Some data were obtained for Mach numbers below 4.9. These tests were made in the NOL Aerophysics Tunnel No. 6, which operates continuously from atmospheric supply at Mach numbers up to 5.

*Technical E Copper Cement (W. V-E Ames Company, Fremont, Ohio) which is useful up to 1000° Kelvin (reference (e)).

RESULTS

6. Detailed performance investigations were made with a circular probe of a vent-area to entrance-area ratio of 1:5 and a thermocouple projection of 2.5 mm (reference (a)). Figure 2 shows the calibration results at various Mach numbers plotted as a function of the free stream Reynolds number, which is based on the probe entrance diameter. Data measured at low Mach numbers are not shown. They correspond to Reynolds numbers above 40,000. Under these conditions the recovery factor was constant and equal to .998. The data presented in this form do not provide usable reference curves for the practical application of stagnation temperature probes, since Mach number as well as temperature seem to be parameters affecting the displacement of the calibration curves. The variation of the recovery factor with temperature alone was investigated at a Mach number of 4.9. Three series of tests were made for the same range of Reynolds numbers at three different supply temperatures, Figure 3. The overall shape of the curves in Figures 2 and 3 appears to be alike. For each Mach number and temperature, the recovery factor decreases with decreasing Reynolds number and does so more rapidly as the temperature is increased. The decrease is caused by the relative increase of the conduction and radiation errors as compared to the convective heat transfer. The thermometric losses have been estimated using the relations for the radiation and conduction errors given in the Appendix. It was found that for this specific type of probe and at the temperatures involved, the major losses are conduction losses. A numerical example is given in the Appendix for the data in the lower portion of the Mach number 7.6 curve (Figure 2). In this case approximately 95 percent of the total losses are due to conduction.

7. Since the deviation of the measured temperature from the true stagnation temperature is essentially determined by the convective heat transfer from the air sample within the shield to the sensing element, and by the temperature losses experienced in the immediate surroundings of the sensing element, the performance of the probe can be related more adequately to conditions of the flow inside the probe rather than to any free-stream parameter. The temperature recovery factor should then be a function of a variable proportional to the convective heat transfer coefficient. The analysis given in the Appendix suggests

$$r = f\left(Nu\frac{k_g}{k_w}\right) \qquad (2)$$

where the Nusselt number refers to the flow conditions inside

the probe and is based on the wire diameter

$$Nu = h_c \frac{D}{k_g} \tag{3}$$

If $Nu\ k_g/k_w$ is the characteristic independent variable, a single calibration curve should describe the performance of a stagnation temperature probe regardless of the free-stream conditions at which the data were obtained. This is borne out in Figure 4, which shows that the data of Figures 2 and 3 fall into a single curve if $Nu\ k_g/k_w$ is used as the independent variable.

8. For use of the calibration data as a reference curve, the variable $Nu\ k_g/k_w$ is an inconvenient term because it is not readily computed from the experimental pressure and temperature data. A more practical variable is obtained by writing the Nusselt number in terms of the Prandtl and Reynolds numbers for the flow inside the probe (for details see the Appendix) and expressing those and the ratio of the thermal conductivities as functions of the temperature and density. The other factors involved are, for one specific probe, constant and can be omitted. Thus

$$(Nu \frac{k_g}{k_w})^2 \sim \rho_3/T_o^{3/4} \tag{4}$$

That $\rho_3/T_o^{3/4}$ is a good approximation for the independent variable is illustrated in Figure 5, which shows the calibration data of one probe (circular probe with $L/D = 10$, Figure 4) plotted as a function of $\rho_3/T_o^{3/4}$.

Effect of Vent Hole Size

9. The effect of the variation of the vent- to entrance-area ratio on the performance of the probe was investigated with a circular probe similar to that shown in Figure 7. Five shields of identical shape and air entrance-area but different vent hole size were used in conjunction with an otherwise unchanged probe. The results of these tests are shown in Figure 6. The temperature recovery factor of probes with vent- to entrance-area ratios of 1:4 and larger remained constant and equal to .998 for values of $Nu\ k_g/k_w$ larger than 3×10^{-3}. With decreasing vent- to entrance-area ratio, however,

the probe performance becomes less desirable. The recovery factor decreases with decreasing Nu k_g/k_w, the decrease being most pronounced for the probe with the smallest area ratio.

10. The flow Mach number inside the probe for all five shields is low and varies between M = .07 and .155. The recovery errors can be considered still negligibly small. The decrease of the probe performance probably can be attributed to increased conduction losses; therefore, probes built subsequently have vent- to entrance-area ratios of 1:4 or larger.

Variation of Shield Design

11. The three shield designs used are shown in Figure 7. One is a circular shield with the entrance and the overall shape circular, as described before. The second is a two-dimensional probe* which has a shield made of steel with all exposed surfaces gold plated. The air entrance as well as the vents are narrow slots. In order to expose a sufficient length of the 38 gauge thermocouple wire within the limited enclosed space of the shield, the thermocouple is mounted in cross-flow with the leads coming out on both sides near the air entrance where they are cemented to the exterior of the shield on its narrow sides. The slender shape and the thin walls of the shield permit measurements close to solid boundaries ($y \simeq .2$ mm). At low total pressures ($p_o' \sim 50$ mm Hg and less), the mechanical performance of the probe is satisfactory; however, with increasing p_o' the shield begins to deform and the temperature readings fluctuate widely. Wall interferences with this rather wide probe and the deformation of the shield limited the measurement closest to a wall to .5 mm. The third probe has a circular shield with rectangular air entrance and is made of silica which is platinum coated. The entrance is collapsed to a narrow slot of .8 x 5 mm inside dimensions; the vent holes are circular and are drilled through the steel body of the shield support. A swivel arrangement of the shield support provides for alignment of the shield. Measurements can be made to .5 mm from a wall.

12. Comparative tests of the probes with the three shield designs did not show any effect of the shield shape on the performance of the probe. In the temperature range of the investigations (up to 800° K) and with the shields carefully insulated from their supports, thermometric losses due to

---

*This probe was designed by M. Sibulkin, formerly at NOL but presently at the Jet Propulsion Laboratory, Los Angeles, California.

conduction through the shield and radiation from their surfaces seem to be negligible. This is illustrated by the curve marked "circular and two-dimensional" in Figure 8 which gives the performance of both a silica platinum-coated shield and the steel gold-coated shield.

Variation of Thermocouple Projection

13. Since the estimation of the thermometric losses of the probes (see Appendix) indicated that the major losses are due to conduction in the thermocouple wires, increasing the length-over-diameter ratio of the thermocouple wire above the L/D = 10 of the original probe should result in improved performance over a wider range of flow conditions. The L/D ratio was increased up to 50. With the shorter projection lengths a simple loop arrangement of the thermocouple was used. For the longer projections, the thermocouple was wound into a helix with its axis parallel to the probe axis. With increasing L/D ratio a constant performance is achieved over a wider range of flow conditions, and also the decrease of the probe temperature recovery factor with decreasing Nu k_g/k_w becomes less pronounced. A summary of the results is given in Figure 8.

Reduction in Size

14. Two probes, smaller than mentioned before, were manufactured. One, a circular probe, Figure 9, differs in its design from that of the previously discussed probes in one feature. A single vent hole is provided in order to simplify assembly. Venting is done through a fine silica tube positioned in the center of the shield support. The thermocouple wires are cemented to the exterior of this vent tube, and this arrangement is then sealed into the shield support which is provided with holes of arbitrary size to release the air. The other probe is a scaled-down version of the large rectangular-round probe (Figures 10 and 11) but with an L/D ratio of 100.

15. The performance of the two small probes is shown in Figure 12 together with some of the data of the large rectangular-round probe (Figure 8). For values of Nu k_g/k_w in excess of $.9\times10^{-3}$, the performance of the small rectangular-round probe is comparable to that of the larger probe. The increased value of the probe temperature recovery factor is of a magnitude to be expected for an L/D ratio of 100. The performance of the single-vent probe, however, in the same range of abscissa values, is less desirable than that of other probes with comparable L/D ratios and vent- to entrance-area ratios. The rather steep decrease of the recovery factor of both small

probes for abscissa values below $.9\ 10^{-3}$ and $1.1\ 10^{-3}$, respectively, cannot be explained by conduction errors (radiation errors are negligibly small in either case) unless a change in the flow condition inside the probes invalidates the calculation of $Nu\ k_g/k_w$ in the simple fashion indicated in the Appendix.

Recommended Data Reduction Procedure

16. In the practical application of stagnation temperature probes, local flow properties are determined from the measured temperature, T_i, the temperature recovery factor of the probe, and the local Mach number as calculated from measured static and pitot pressures. The local true stagnation temperature T_o is calculated from the measured quantities using

$$T_o = \frac{T_i}{r + (1 - r)\left[1 + \frac{\gamma - 1}{2} M^2\right]^{-1}} \qquad (5)$$

which follows from the definition of the recovery factor (equation (1)). Since the recovery factor to be inserted in the above equation depends on the unknown flow properties ρ_3 and T_o at the measuring station (equations 2 and 4), the following iteration process is applied. The density inside the probe is replaced by p_2/RT_i, where p_2, the pressure behind the bow wave in front of the probe, can be computed from the Mach number and the measured pitot pressure. With the recovery factor corresponding to $p_2/RT_i^{7/4}$ read from the calibration curve, a T_o is computed by equation (5). This T_o and a ρ_3 computed from pitot pressure and T_o are then used in the second iteration. In all practical cases, however, it was found that the first iteration already yielded T_o values within less than 1 percent of its true value, which is within the accuracy of the other experimental data.

Use of Probes for Turbulent Boundary Layer Surveys

17. In the investigations of the turbulent boundary layers at the nozzle wall of the hypersonic tunnel (reference (d)) the probes with rectangular-round shields were used to determine the stagnation temperature variation across the boundary layer. These data, together with measured static and pitot pressures, made it possible to evaluate the static temperature and the velocity profiles. The small height at

the air entrance of these probes facilitated the measurement of temperatures in the laminar sublayer and the computation of boundary layer parameters from the experimental data.

SUMMARY

18. Single-shielded stagnation temperature probes were designed and constructed for use at high supersonic speeds and elevated temperature. They were tested over a wide range of flow conditions, $1.5 \leq M_\infty \leq 7.6$, T_o up to 800^o K, 10^4 cm$^{-1} \leq Re_\infty/x \leq 3\ 10^5$ cm^{-1}.

19. With the shield and thermocouple support made of silica (or other material of low thermal conductivity) and platinum or gold coated on all exposed surfaces, the major thermometric losses of the probes are conduction losses.

20. The performance of any one probe can be described by a single calibration curve if the data are referred to the flow conditions inside the shield. The characteristic independent variable is $Nu\ k_g/k_w$.

21. For large values of $Nu\ k_g/k_w$ the probe temperature recovery factor reaches .998. It decreases as $Nu\ k_g/k_w$ decreases.

22. Vent- to entrance-area ratio, length to diameter ratio of the thermocouple wire, and the physical arrangement of the vent holes are parameters which affect the performance of this specific type of probe.

23. Best performance was found for vent- to entrance-area ratio of 1:4 to 1:5.

24. Use of a single vent hole positioned at the thermocouple support considerably decreased the performance of the probe.

25. With increasing length to diameter ratio of the thermocouple wire, the probe attains a constant recovery factor of .998 for a wider range of $Nu\ k_g/k_w$. The decrease of the recovery factor from its maximum value becomes less pronounced.

26. The obtaining of a single calibration curve as a function of $Nu\ k_g/k_w$ reduces the number of data needed to know the performance of a probe for any range of flow conditions (as long as radiation errors remain negligibly small).

27. The use of the total temperature probe together with static pressure and pitot pressure measurements, makes it possible to evaluate flow data without resorting to assumptions.

28. Probes of 1 mm height at the air entrance were successfully used to determine the temperature variations across turbulent boundary layers, and in particular to obtain data in the laminar sublayer. These measurements were made in boundary layers of approximately 1 inch total thickness in the Mach number range 5 to 8.

REFERENCES

(a) Winkler, E. M., "Design and Calibration of Stagnation Temperature Probes for Use at High Supersonic Speeds and Elevated Temperatures," J. Appl. Phys. 25, 221 (1954).

(b) Wegener, P. P., "Summary of Recent Experimental Investigations in the NOL Hyperballistics Wind Tunnel," J. Aeronaut. Sci. 18, 665 (1951).

(c) A discussion of stagnation temperature probes and additional references can be found in:

Goldstein, D. U. and Scherrer, R., "Design and Calibration of a Total Temperature Probe for Use at Supersonic Speeds," NACA TN 1885 (1945).

Eber, G. R., "Shielded Thermocouples," High Speed Aerodynamics and Jet Propulsion, Volume IX - Physical Measurements in Gas Dynamics and Combustion, Princeton University Press, 1954.

(d) Lobb, R. K.; Winkler, E. M.; and Persh, Jerome, "Experimental Investigation of Turbulent Boundary Layers in Hypersonic Flow," presented at the 22nd Annual Meeting of the Institute of the Aeronautical Sciences, January 1954, Preprint 452.

(e) Souder and Paffenbarger, N. B. S. Circular C 433, p. 96.

(f) Winkler, E. M., "NOL Hypersonic Tunnel No. 4, Results IV, High Supply Temperature Measurement and Control," NAVORD Report 2574 (1952).

(g) Burcher, Marie A., "Compressible Flow Tables for Air," NACA TN 1592 (1948).

(h) Scadron, M. D.; Warshawsky, I., "Experimental Determination of Time Constant and Nusselt Numbers for Bare Wire Thermocouples in High Velocity Air Streams and Analytical Approximation of Conduction and Radiation Errors," NACA TN 2599 (1952).

(i) Eckert, E. R. G., "Introduction to the Transfer of Heat and Mass," McGraw Hill, New York (1950).

APPENDIX A

Estimation of Thermometric Losses and Time Constant

1. The temperature indicated by a stagnation temperature probe can be found from a balance of the heat transferred to the sensing element by convection from the air sample within the shield, the radiative heat exchange between the thermocouple and the surrounding surfaces (as given by the Stefan-Boltzmann law), and the conduction heat transfer from the thermocouple to its support and that across the shield wall. This balance leads to an expression for the true gas temperature as the sum of the measured temperature and correction terms which account for the thermometric losses. A detailed discussion of the heat balance equation for bare-wire thermocouples in low velocity air streams is given in reference (h), from which the following equation was taken (equation C13 in reference (h)).

$$T_o = T_i + \beta\left[(1 - \varepsilon_g) - (1 - \alpha_{g,d})\left(\frac{T_d}{T_i}\right)^4\right] + (T_i - T_b)\frac{\gamma}{1-\gamma} \quad \text{(A1)}$$

where the terms

$$\beta\left[(1 - \varepsilon_g) - (1 - \alpha_{g,d})\left(\frac{T_d}{T_i}\right)^4\right] \quad \text{(A2)}$$

$$(T_i - T_b)\frac{\gamma}{1-\gamma} \quad \text{(A3)}$$

represent the radiation and conduction errors, respectively, with

$$\beta = \sigma\, \varepsilon_w\, T_i^4/h_c \quad \text{(A4)}$$

$$\gamma = \operatorname{sech}\left[(h_c L^2/Dk_w)^{\frac{1}{2}}\right] \quad \text{(A5)}$$

2. To apply the above equations to the calculation of the conduction and radiation errors of a shielded stagnation temperature probe, the following assumptions were made with respect to the support and shield temperatures T_b and T_d: (a) $T_b = T_d$; (b) T_d, the inside surface temperature of the shield is identified with a temperature of a value between the equilibrium recovery temperatures of the interior and exterior shield surfaces. To obtain a numerical value for T_d, a heat balance like that underlying equation (A1) applies. For the present case, the calculations can be simplified because radiation losses from the platinum- or gold-coated shields to the cooler wind tunnel walls are negligibly small, at least in the temperature range where the probes were used. In addition, the conduction losses from the shield to the probe support were neglected because the temperature difference between shield and support can be assumed to be small, and also because of the thermal insulation used between shield and support. The shield temperature was therefore determined from an estimate of the forced convection heat transfer to the inner surface and an assumed equilibrium value of the exterior surface temperature of

$$Te = Pr^{\frac{1}{2}} (T_o - T_\infty) + T_\infty \qquad (A6)$$

3. The time constant can be computed from the following relation (equation C12 of reference (h))

$$\tau = \frac{D \rho_w c_w / 4 h_c}{1 + 4 \beta \varepsilon_g / T_i} \qquad (A7)$$

With the help of the charts of reference (h), the thermometric losses and time constants were determined. An example is given for the following flow conditions and probe data:

$M_\infty = 7.60$	$T_o = 650^\circ$ K	Flow Data
$p_o = 10$ atm	$Te = 560^\circ$ K	
$M_3 = .08$	$T_i = 599^\circ$ K	
$p_3 = .108$ atm	$T_d = 590^\circ$ K	
$D = .25$ mm	$T_o - T_i = 51^\circ$ K	Probe Data
$L/D = 10$	$r = .915$	
$\varepsilon_w = .75$		

Radiation error:

$$\beta = 18.8^{\circ} \text{ K}$$

$$\Delta T_{rad} \simeq \beta\left[1 - \left(\frac{T_d}{T_i}\right)^4\right] = 1.1^{\circ} \text{ K}$$

or 2 percent of the observed $T_o - T_i$

Conduction error:

$$\gamma = .845$$

$$T_i - T_d = 9^{\circ} \text{ K}$$

$$\Delta T_{cond} = \frac{\gamma}{1 - \gamma} (T_i - T_d) = 49^{\circ} \text{ K}$$

or 96 percent of observed $T_o - T_i$

Time constant:

$$\tau = .58 \text{ sec.}$$

The Independent Variable of the Calibration Curve

5. The relative importance of the conduction losses in comparison to the radiation error suggests that, in a temperature range where the latter remains small, the temperature recovery factor of the probe can be represented as a function of the convection heat transfer coefficient h_c and the thermal resistance of the thermocouple wire D/k_w

$$r = f\,(h_c\, D/k_w) \qquad \text{(A8)}$$

where h_c refers to the heat transfer from the air sample within the shield to the thermocouple wire. (A8) can be derived from (A1) and (A5) if the radiation losses are neglected and T_b is set equal to the equilibrium recovery temperature of the shield as given by (A6). Expressing h_c

in terms of the Nusselt number of the flow inside the shield

$$h_c = Nu^{k_g} \tag{A9}$$

the argument of equation (A8) becomes

$$h_c \frac{D}{k_w} = Nu \frac{k_g}{k_w} \tag{A10}$$

6. For practical purposes, however, it was found more convenient to express (A10) in terms of the variable flow properties ρ_3 and T_o, and to omit those factors which are constant for one specific probe. Considering the thermocouple wires as cylinders in cross flow, the Nusselt number is (reference (i))

$$Nu = \text{const } Re^{\frac{1}{2}} Pr^{1/3} \tag{A11}$$

where the Reynolds number is based on the wire diameter. With

$$u = (\gamma R T_o)^{\frac{1}{2}} M_3 = \text{const } T_o^{\frac{1}{2}} \tag{A12}$$

$$\mu = \mu_{ref} \left(\frac{T_o}{T_{ref}}\right)^{.76} = \text{const } T_o^{.76} \tag{A13}$$

$$k_g = (k_g)_{ref} \left(\frac{T_o}{T_{ref}}\right)^{.78} = \text{const } T_o^{.78} \tag{A14}*$$

---

*This form was recommended by E. R. G. Eckert

we have

$$Pr = \text{const } T_o^{-.02} \tag{A15}$$

$$Re = \text{const } \rho_3 T_o^{-.26} \tag{A16}$$

and

$$Nu = \text{const } \rho_3^{\frac{1}{2}} T_o^{-.14} \tag{A17}$$

Finally, assuming that the thermal conductivity of the wire is simply proportional to the temperature

$$k_w = \text{const } T_o \tag{A18}$$

equation (A10) can be written as

$$Nu \frac{k_g}{k_w} = \text{const } \rho_3^{\frac{1}{2}} T_o^{-.36} \tag{A19}$$

On the basis of this relation $(\rho_3^{\frac{1}{2}} T_o^{-.36})^2 \simeq \rho_3 / T_o^{3/4}$ is selected as the independent variable for plotting calibration data used as reference in the practical application of the probes.

Notes on the Manufacture of the Probes

7. The following procedure was used in the manufacture of the shields: A silica or Vycor* tube is first drawn to the specified fine wall thickness. The section which is used for

*Vycor, (Corning Glass Works, Corning, New York) Trade name for high silica glass, 96 percent SiO_2, 3 percent B_2O_3, 1 percent oxides.

the inlet is then drawn out to a fine tip and sealed off. Positioning this piece vertically with the sealed end down, a carbon mandrel machined accurately to the specified shape of the shield is then inserted and the open end connected to a good vacuum. By heating the section where the mandrel is inserted, working gradually from the tip to the wider section, the silica or Vycor collapses accurately around the mandrel. After cooling the mandrel can be removed without difficulty. The probe ends are then cut and fire-polished.

8. The vent holes were ground in the silica shields using a jewelers lathe, the shaft ends of drills as the tools, and a fine-grid diamond lapping compound. By carefully adjusting the pressure applied while grinding, it was unnecessary to fill the shield interior with a wax mandrel. This aided in aligning the vent holes.

9. The platinum plating was done with Liquid Bright Platinum No. 05 (Hanovia Chemical & Manufacturing Company, Newark, New Jersey) according to manufacturer's directions.

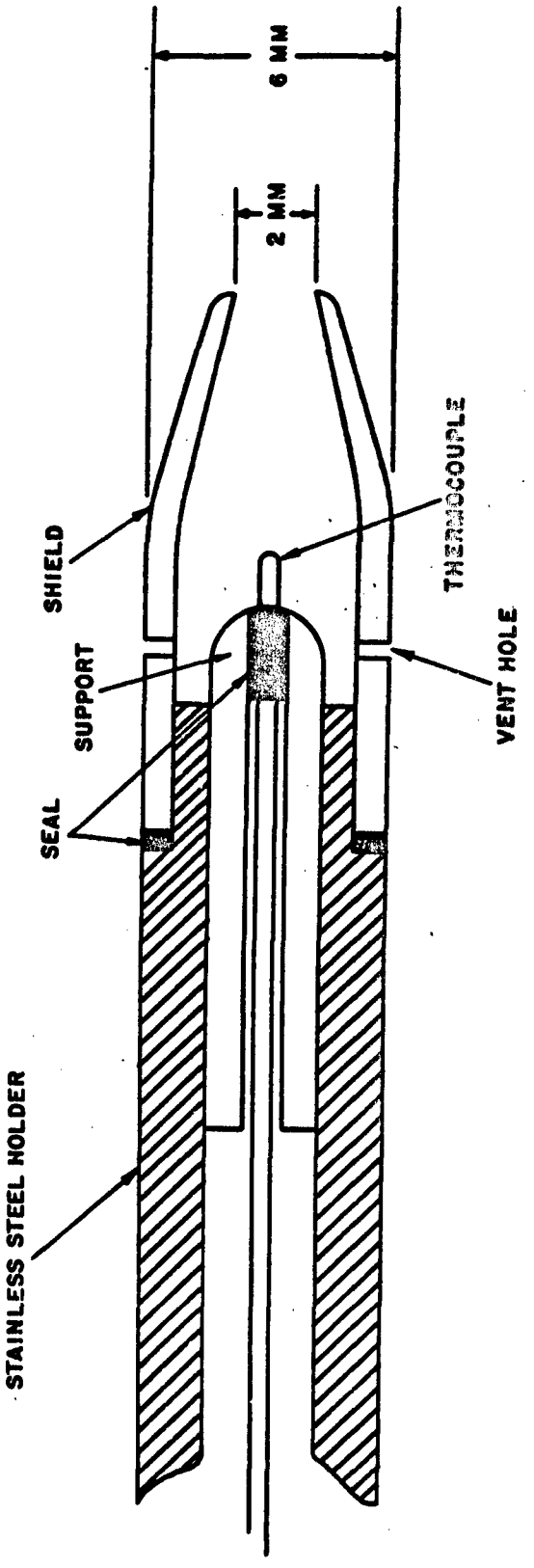

FIG. 1 DESIGN OF STAGNATION TEMPERATURE PROBE

THERMOCOUPLE SUPPORT AND SHIELD MADE OF SILICA WITH ALL EXPOSED SURFACES PLATINUM COATED;
THERMOCOUPLE: IRON–CONSTANTAN, 0.25 MM DIAMETER, FIBERGLAS INSULATED;
TWO VENT HOLES;

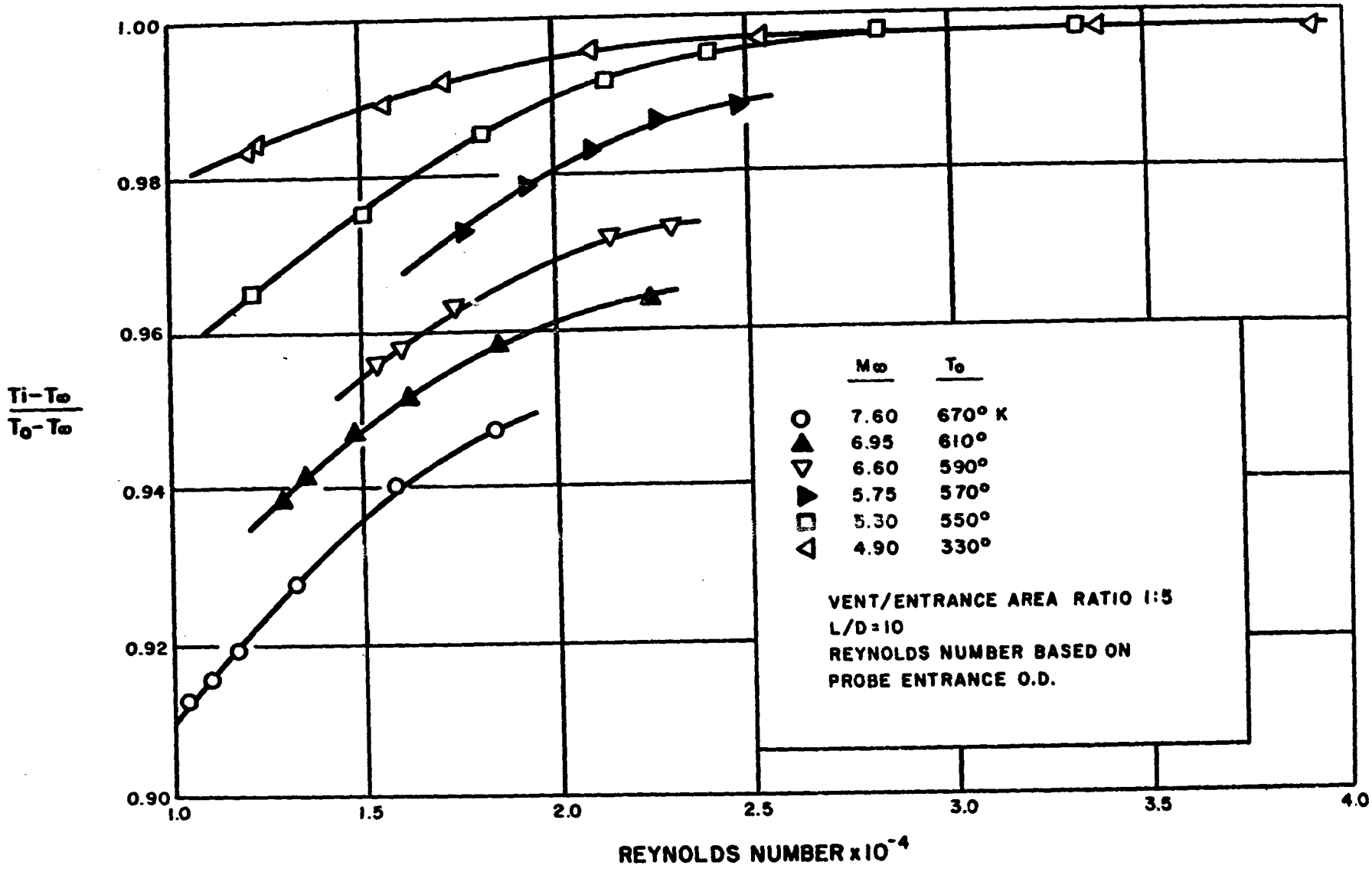

FIG. 2 VARIATION OF PROBE TEMPERATURE RECOVERY FACTOR WITH FREE-STREAM REYNOLDS NUMBER AT VARIOUS FREE STREAM MACH NUMBERS

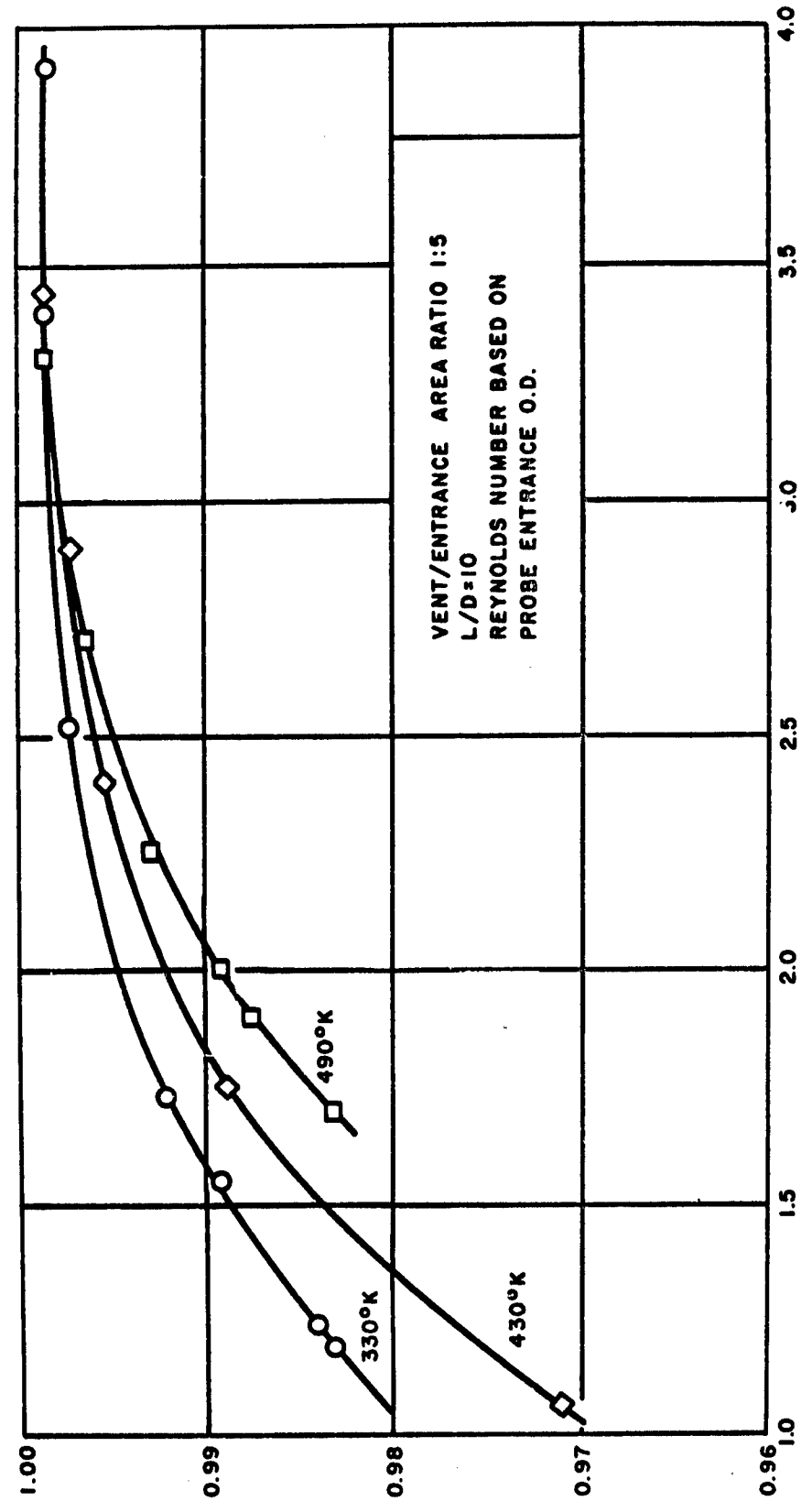

FIG. 3 VARIATION OF PROBE TEMPERATURE RECOVERY FACTOR WITH FREE-STREAM REYNOLDS NUMBER AT THREE DIFFERENT STAGNATION TEMPERATURES FOR A FREE STREAM MACH NUMBER OF 4.90

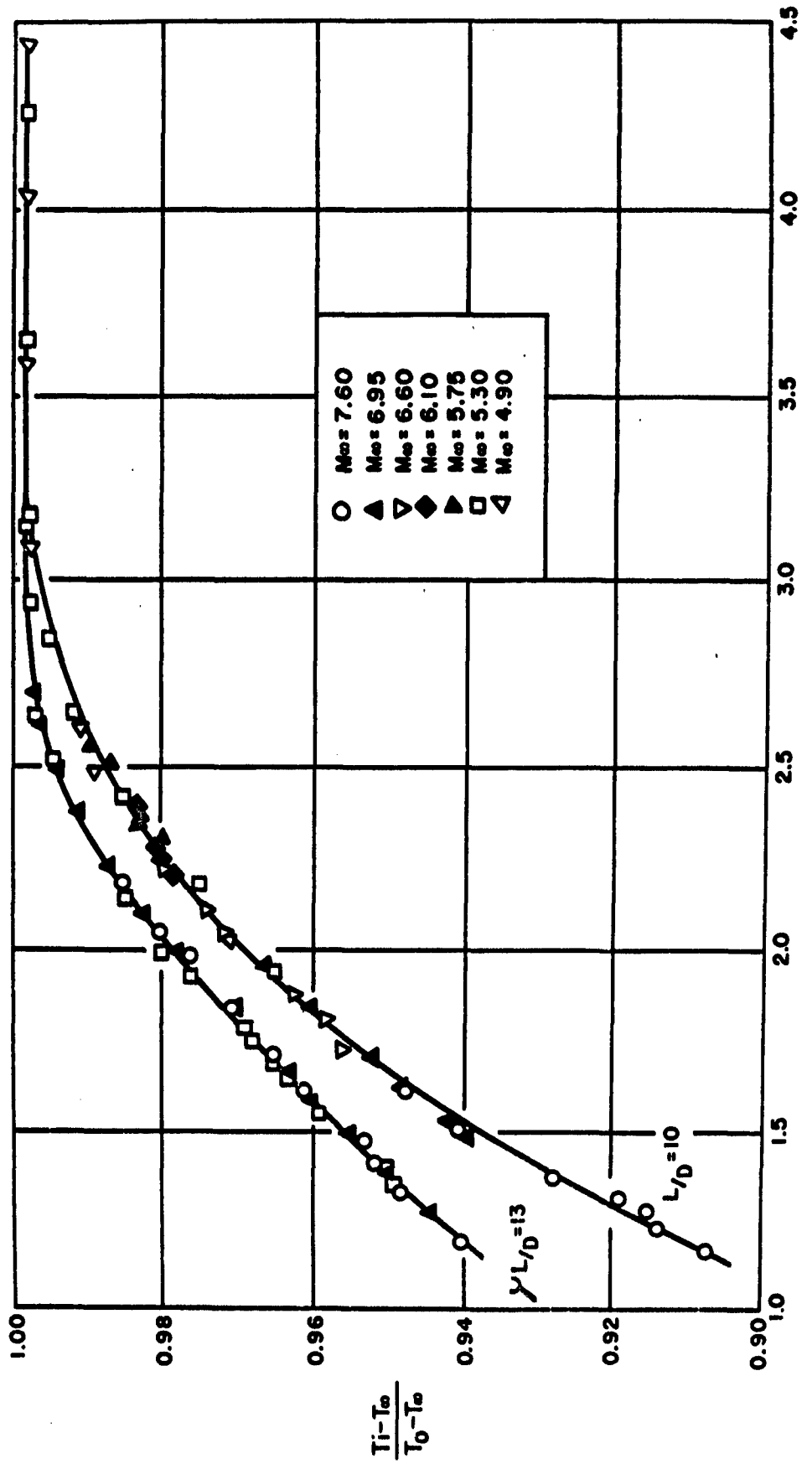

FIG. 4 SUMMARY OF CALIBRATION DATA FOR TWO PROBES

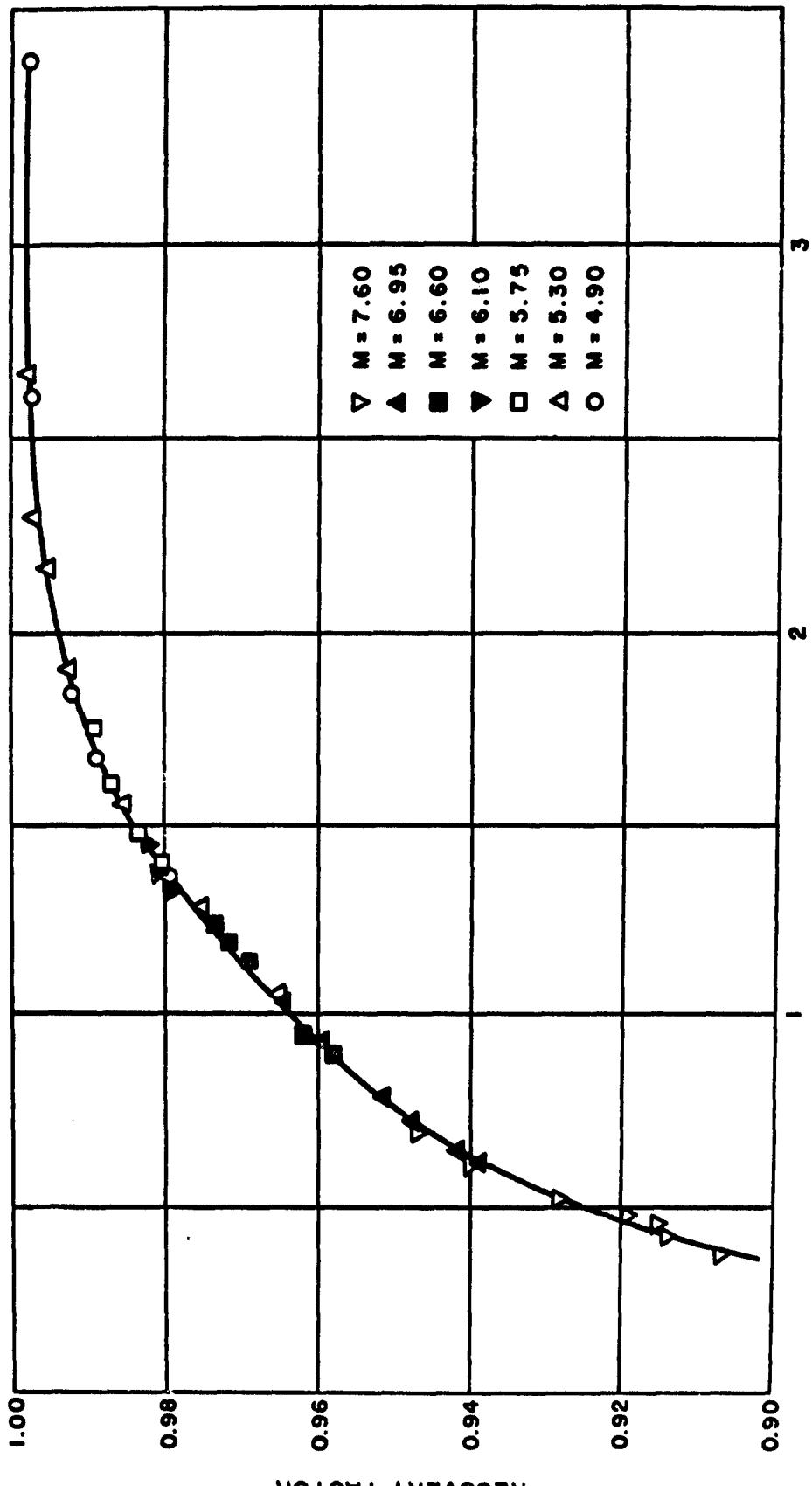

FIG. 5 CALIBRATION DATA FOR ONE PROBE AS FUNCTION OF $\rho_3/T_0^{3/4}$

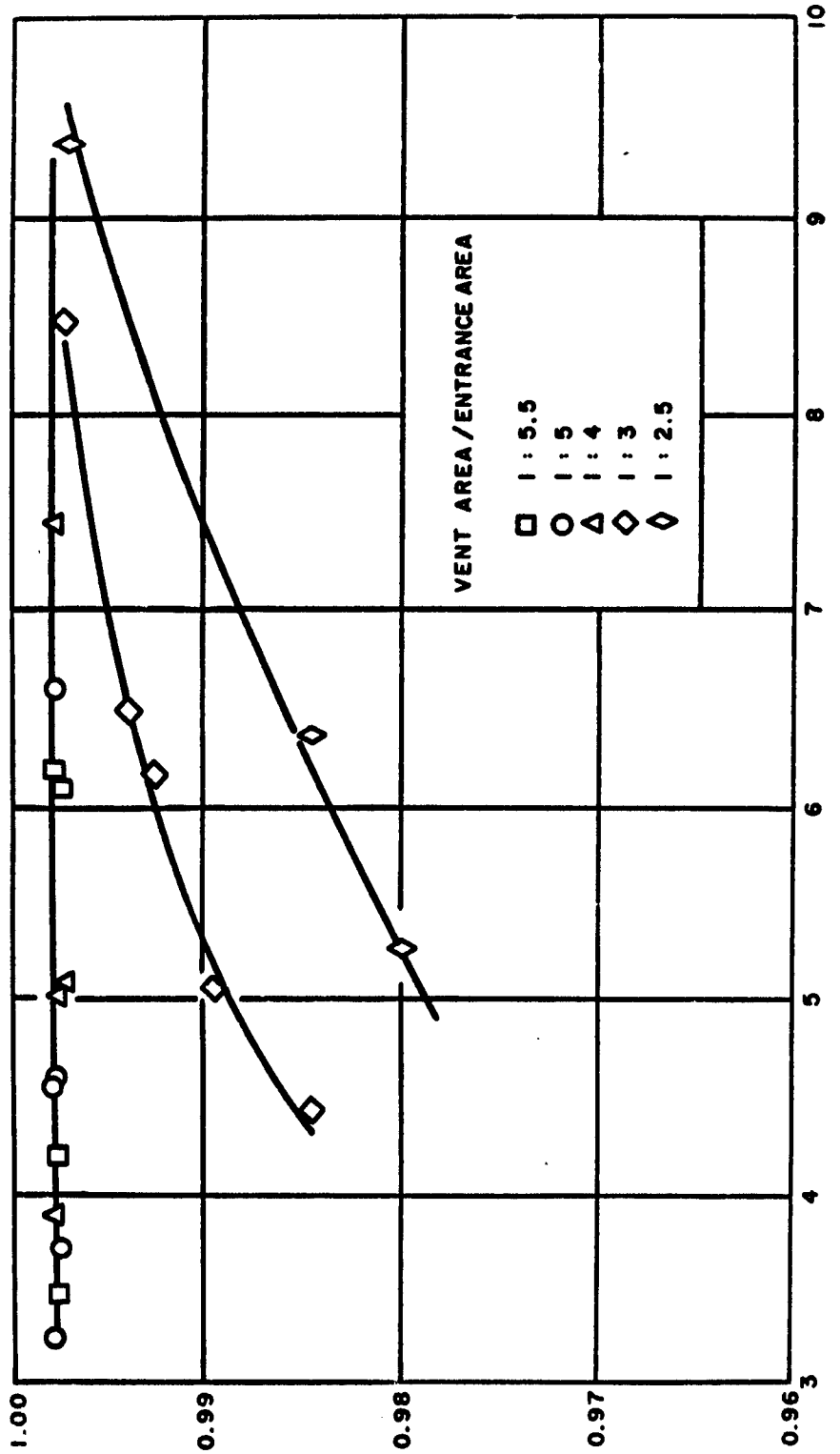

FIG. 6 VARIATION OF PROBE PERFORMANCE WITH VENT-TO ENTRANCE-AREA RATIO

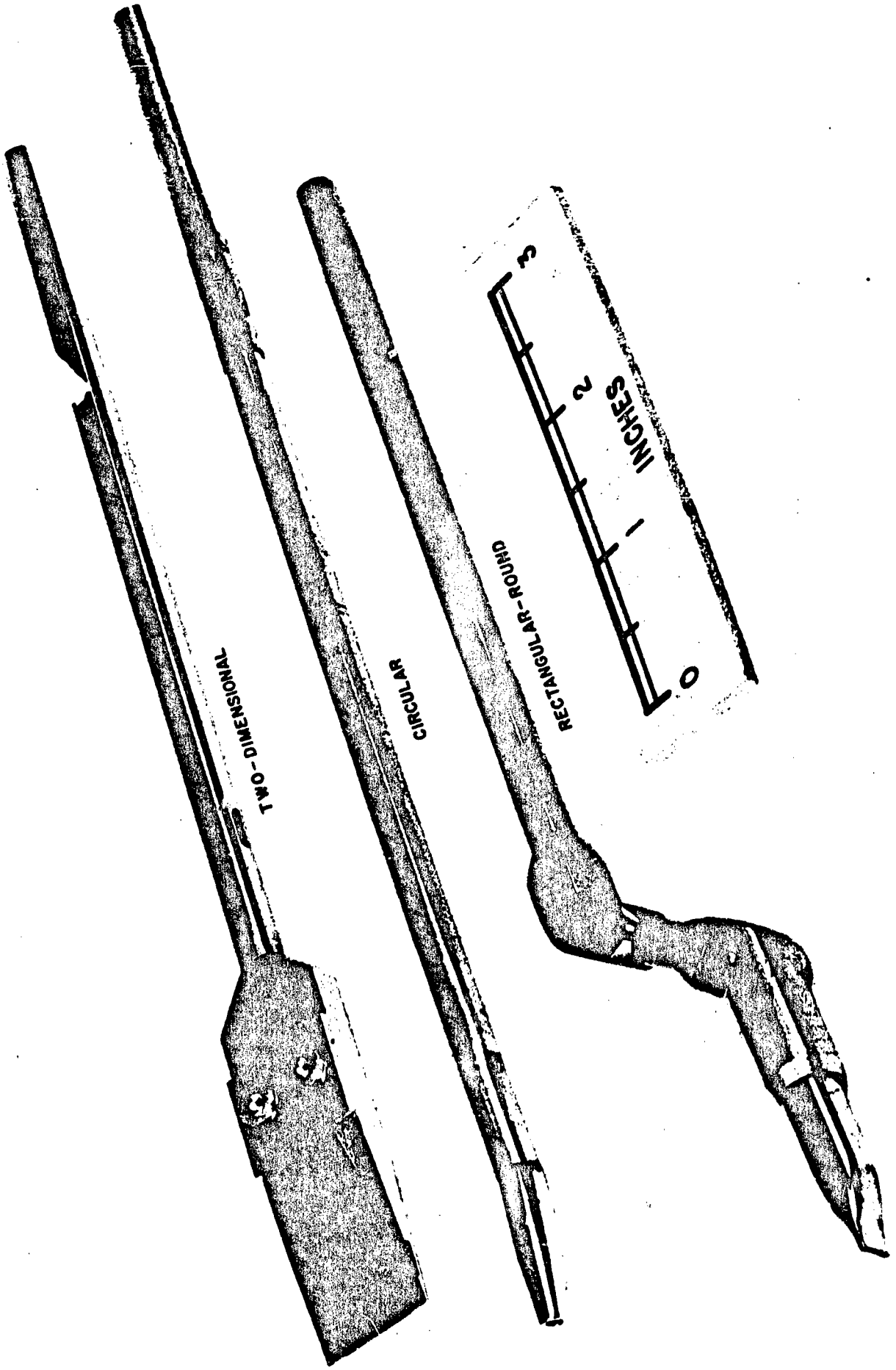

FIG. 7 PROBES WITH THREE DIFFERENT SHIELD DESIGNS

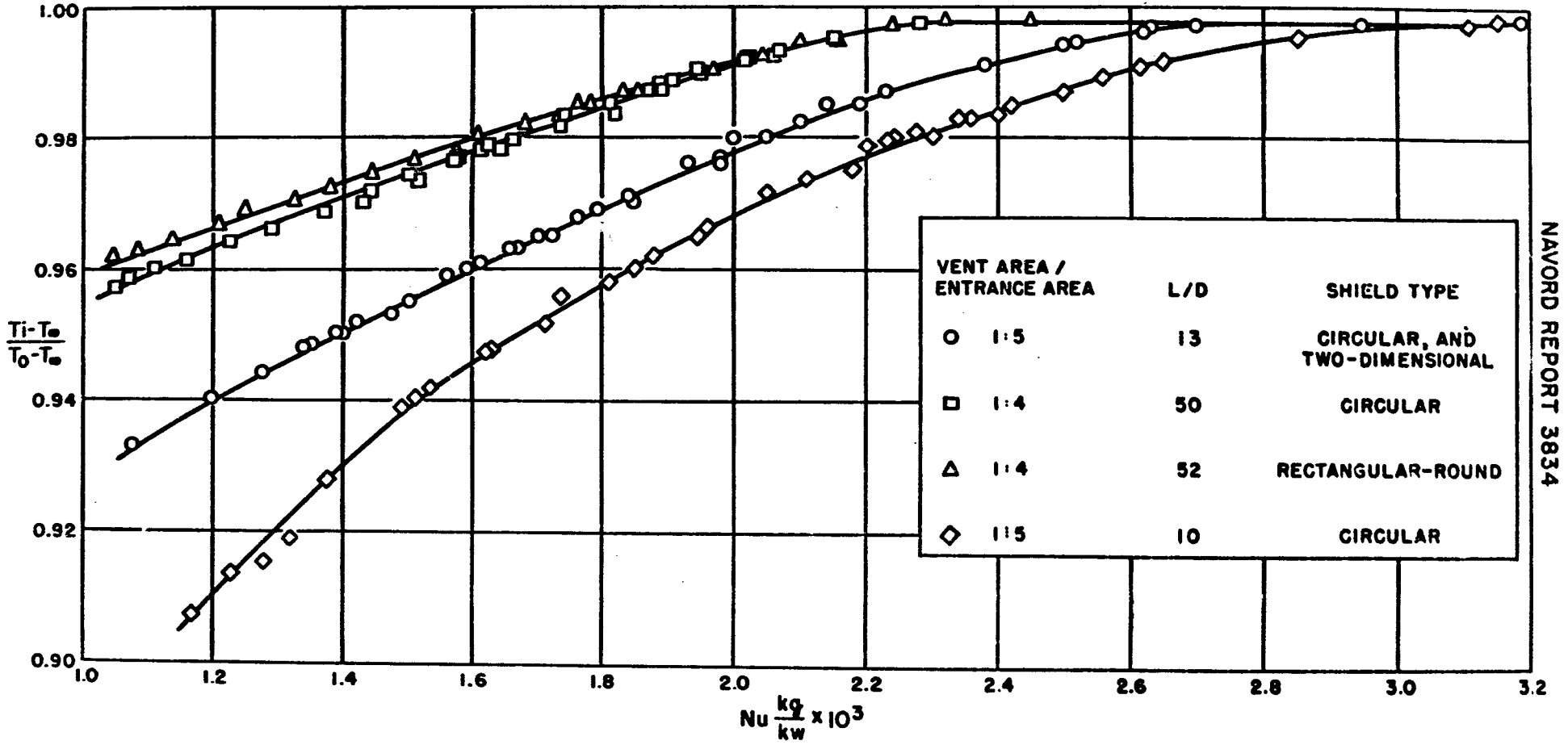

FIG. 8 SUMMARY OF CALIBRATION DATA FOR FIVE PROBES

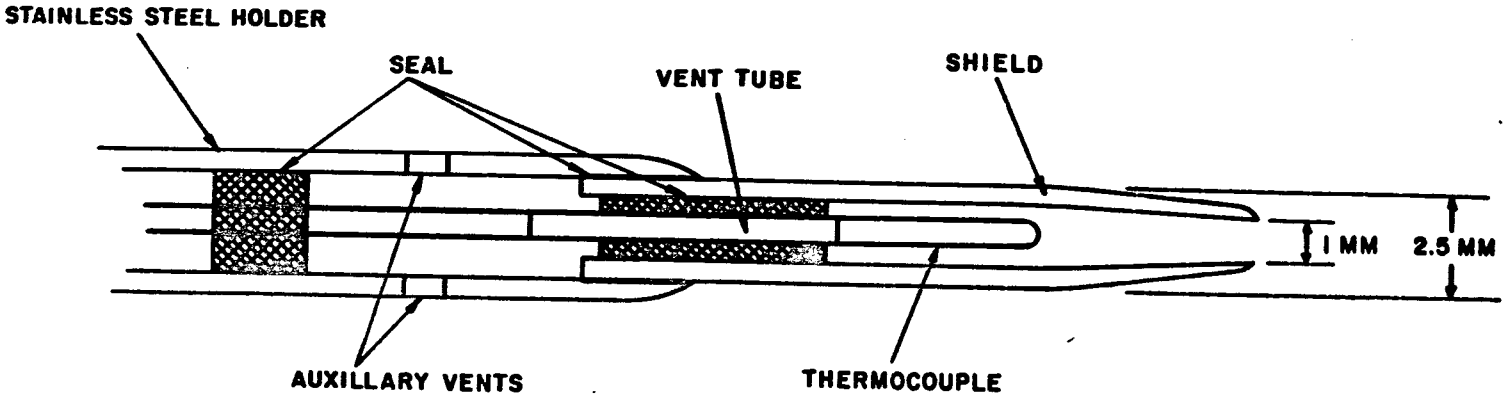

FIG. 9 DESIGN OF SMALL CIRCULAR PROBE

SHIELD MADE OF SILICA WITH ALL EXPOSED SURFACES PLATINUM COATED;
VENT TUBE MADE OF SILICA, 0.5 MM I.D.;
THERMOCOUPLE: IRON-CONSTANTAN, 0.25 MM DIAMETER,

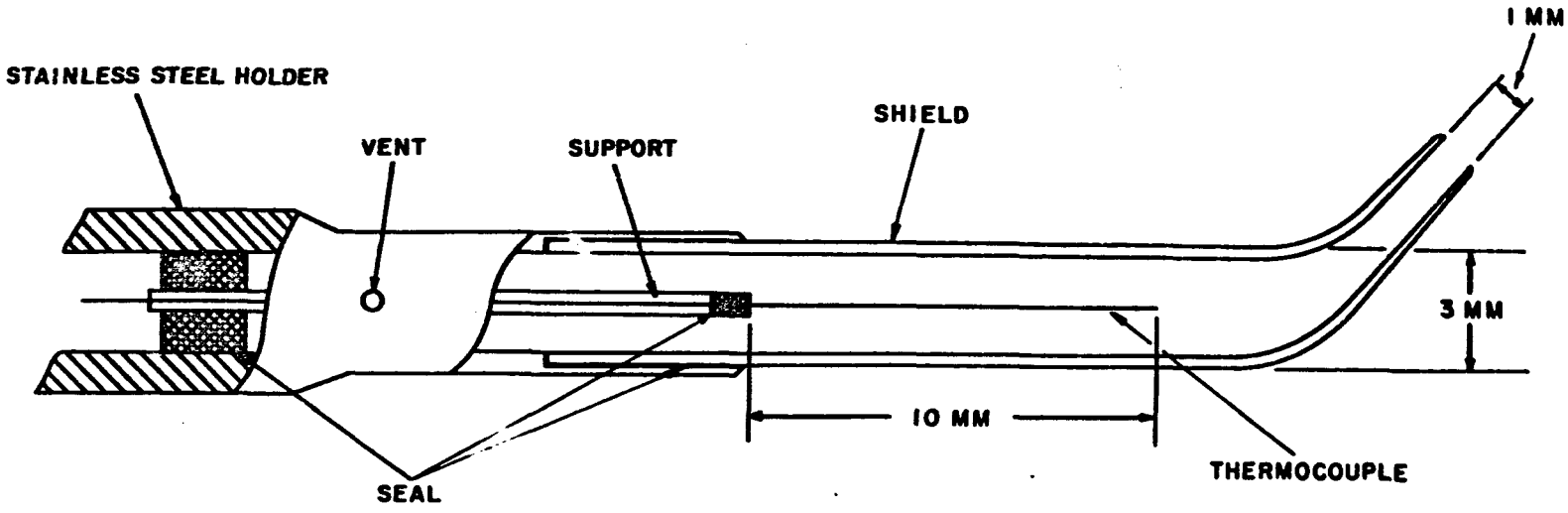

FIG. 10 DESIGN OF SMALL RECTANGULAR–ROUND PROBE

THERMOCOUPLE SUPPORT AND SHIELD MADE OF VYCOR WITH ALL EXPOSED SURFACES PLATINUM COATED;
THERMOCOUPLE: IRON-CONSTANTAN, 0.10 MM DIAMETER;
AIR ENTRANCE: 2.5 MM BY 1 MM;
THERMOCOUPLE LOOP PERPENDICULAR TO CROSS-SECTION SHOWN;

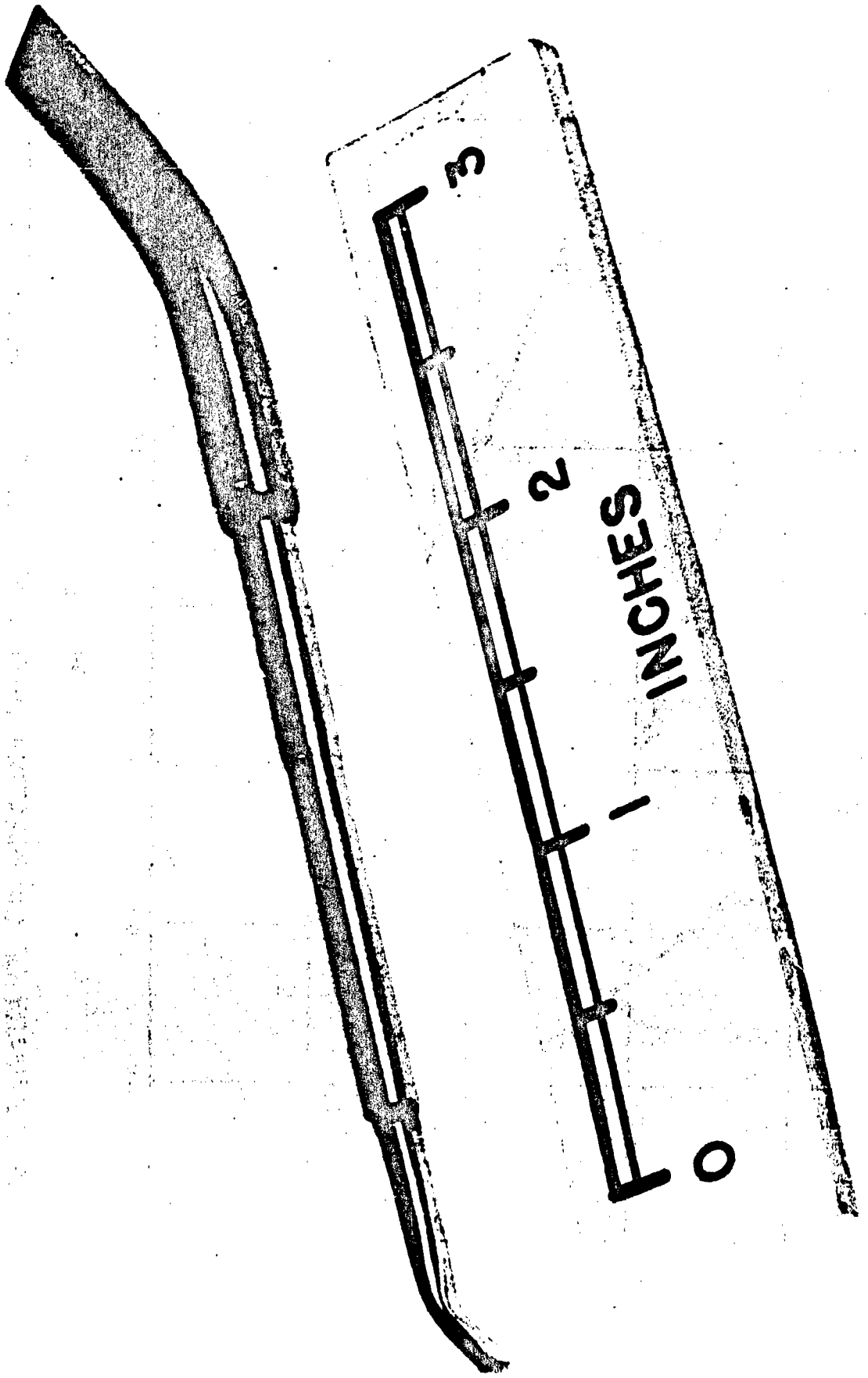

FIG. 11 SMALL RECTANGULAR-ROUND PROBE

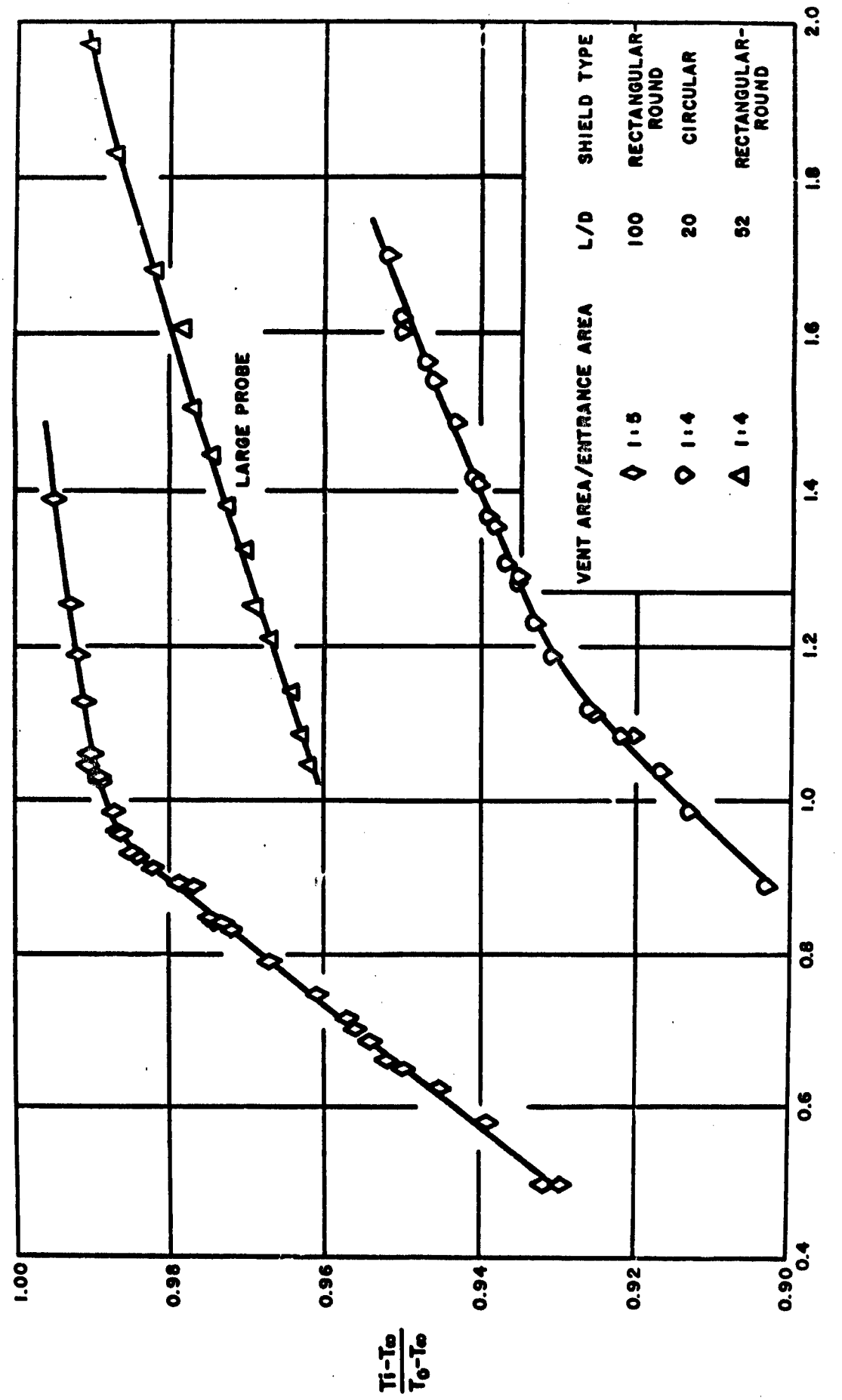

FIG. 12 SUMMARY OF CALIBRATION DATA FOR THE TWO SMALL PROBES AND COMPARISON WITH THE DATA FOR ONE LARGE PROBE

Aeroballistic Research Department
External Distribution List for Aeroballistics Research (XI)

No. of Copies	
	Chief, Bureau of Ordnance Department of the Navy Washington 25, D. C.
1	Attn: Re3d
2	Attn: Re6
2	Attn: Re9a
	Chief, Bureau of Aeronautics Department of the Navy Washington 25, D. C.
1	Attn: AER-TD-414
2	Attn: RS-7
	Commander U. S. Naval Ordnance Test Station Inyokern P. O. China Lake, California
2	Attn: Technical Library
1	Attn: Code 5003
	Commander U. S. Naval Air Missile Test Center Point Mugu, California
2	Attn: Technical Library
	Superintendent U. S. Naval Postgraduate School Monterey, California
1	Attn: Librarian
	Commanding Officer and Director David Taylor Model Basin Washington 7, D. C.
2	Attn: Hydrodynamics Laboratory
	Chief of Naval Research Library of Congress Washington 25, D. C.
2	Attn: Technical Info. Div.
	Office of Naval Research Department of the Navy Washington 25, D. C.
1	Attn: Code 438
2	Attn: Code 463

No. of Copies	
	Director Naval Research Laboratory Washington 25, D. C.
1	Attn: Code 2021
1	Attn: Code 3800
	Office, Chief of Ordnance U. S. Army Washington 25, D. C.
1	Attn: ORDTU
2	Library Branch Research and Development Board Pentagon 3D1041 Washington 25, D. C.
	Chief, AFSWP P. O. Box 2610 Washington 25, D. C.
1	Attn:Technical Library
1	Chief, Physical Vulnerability Branch Air Targets Division Directorate of Intelligence Headquarters, USAF Washington 25, D. C.
	Commanding General Wright Air Development Center Wright-Patterson Air Force Base Dayton, Ohio
5	Attn: WCACD
1	Attn: WCSD
2	Attn: WCSOR
2	Attn: WCRRN
1	Attn: WCACD
1	Attn: WCRRF
2	Attn: WCLGH
1	Director Air University Library Maxwell Air Force Base, Alabama

No. of Copies

Commanding General
Aberdeen Proving Ground
Aberdeen, Maryland
1 Attn: C. L. Pocr
1 Attn: D. S. Dederick

National Bureau of Standards
Washington 25, D. C.
1 Attn: Nat'l Applied Math. Lab.
1 Attn: Librarian (Ord.Dev.Div.)
1 Attn: Chief, Mechanics Div.

National Bureau of Standards
Corona Laboratories (Ord. Dev. Div.)
Corona, California
1 Attn: Dr. H. Thomas

University of California
211 Mechanics Building
Berkeley 4, California
1 Attn: Mr. G. J. Maslach
1 Attn: Dr. S. A. Schaaf

2 Commanding General
Redstone Arsenal
Huntsville, Alabama
Attn: Tech. Library

1 Jet Propulsion Lab.
California Institute of Technology
4800 Oak Grove Drive
Pasadena 3, California
Attn: F. E. Goddard, Jr.

California Institute of Technology
Pasadena 4, California
2 Attn: Librarian (Guggenheim Aero Lab)
1 Attn: Dr. H. T. Nagamatsu
1 Attn: Prof. M. S. Plesset
1 Attn: Dr. Hans W. Liepmann
VIA: BuAer Representative

University of Illinois
20. E. E. R. L.
Urbana, Illinois
1 Attn: Prof A. H. Taub

No. of Copies

1 Director
Inst. for Fluid Dynamics and Applied Math
University of Maryland
College Park, Maryland

Massachusetts Inst. of Technology
Cambridge 39, Massachusetts
1 Attn: Prof. G. Stever
1 Attn: Prof. J. Kaye

University of Michigan
Ann Arbor, Michigan
1 Attn: Prof. Otto Laporte

University of Michigan
Willow Run Research Center
Ypsilanti, Michigan
1 Attn: L. R. Biasell

Mechanical Engr.
Univ. of Minn. Bldg.
Minneapolis, Minnesota
1 Attn: Prof. N. Hall

The Ohio State University
Columbus, Ohio
2 Attn: G. L. Von Eschen

Polytechnic Institute of Brooklyn
99 Livingston Street
Brooklyn 2, New York
1 Attn: Dr. Antonio Ferri
VIA: ONR

Princeton University
Princeton, New Jersey
1 Attn: Prof. S. Bogdonoff
VIA: ONR

Massachusetts Inst. of Technology
Cambridge 39, Massachusetts
2 Attn: Project Meteor
1 Attn: Guided Missiles Library

1 Princeton University
Forrestal Research Center Library

Princeton. New Jersy

No. of Copies

Armour Research Foundation
35 West 33rd Street
Chicago 16, Illinois
1 Attn: Engr. Mech. Div.
VIA: ONR

Applied Physics Laboratory
The Johns Hopkins University
8621 Georgia Avenue
Silver Spring, Maryland
1 Attn : Arthur G. Norris
VIA: NIO

1 Cornell Aeronautical Lab., Inc.
4455 Genesee Street
Buffalo 21, New York
VIA: BuAer Rep.

1 Defense Research Laboratory
University of Texas
Box 1, University Station
Austin, Texas

Eastman Kodak Company
50 W. Main Street
Rochester 4, New York
1 Attn: Dr. Herbert Trotter, Jr.
VIA: NIO

General Electric Company
Building #1, Campbell Ave. Plant
Schenectady, New York
1 Attn: Joseph C. Hoffman
VIA: InsMachinery

The Rand Corporation
1700 Main Street
Santa Monica, California
1 Attn: The Librarian

Consolidated Vultee Aircraft Corp.
Daingerfield, Texas
1 Attn: J. E. Arnold
VIA: Dev. Contract Office

Douglas Aircraft Company, Inc.
3000 Ocean Park Boulevard
Santa Monica, California
1 Attn: Mr. E. F. Burton
VIA: Bu Aer Resident Rep.

No. of Copies

1 BuAer Representative
AeroJet--General Corp.
6352 North Irwindale Ave.
Azusa, California

North American Aviation, Inc.
12214 Lakewood Boulevard
Downey, California
2 Attn: Aerophysics Library
VIA: BuAer Representative

United Aircraft Corporation
East Hartford 8, Connecticut
1 Attn: Robert C. Sale
VIA: BuAer Representative

National Advisory Committee for Aero
1724 F Street, Northwest
Washington 25, D. C.
5 Attn: E. B. Jackson

Ames Aeronautical Laboratory
Moffett Field, California
1 Attn: H. J. Allen
2 Attn: Dr. A. C. Charters

NACA Lewis Flight Propulsion Lab
Cleveland Hopkins Airport
Cleveland 11, Ohio
1 Attn: John C. Evvard

Langley Aeronautical Laboratory
Langley Field, Virginia
1 Attn: Theoretical Aerodynamics Div.
1 Attn: J. V. Becker
1 Attn: Dr. Adolf Buseman
1 Attn: Mr. C. H. McLellan
1 Attn: Mr. J. Stack

Harvard University
21 Vanserg Building
Cambridge 38, Massachusetts
1 Attn: Prof. Garrett Birkhoff

The Johns Hopkins University
Charles and 34th Streets
Baltimore 18, Maryland
1 Attn: Dr. Francis H. Clauser

No. of
Copies

New York University
45 Fourth Avenue
New York 3, New York
1 Attn: Professor R. Courant

1 Dr. Allen E. Puckett, Head
Missile Aerodynamics Department
Hughes Aircraft Company
Culver City, California

Acroon, Inc.
385 E. Green Street
Pasadena 1, California
1 VIA: Inspector of Naval Mat'l
1206 S. Santeo Street
Los Angeles 15, Calif.

Engineering Research Inst.
East Engineering Building
1 Ann Arbor, Michigan
Attn: Director of Icing Research

Aeroballistic Research Department
External Distribution List for Aeroballistics Research (XIa)

No. of Copies	
6	Office of Naval Research Branch Office Navy 100 Fleet Post Office New York, New York
	Commanding General Aberdeen Proving Ground Aberdeen, Maryland
1	Attn: Dr. B. L. Hicks
	National Bureau of Standards Aerodynamics Section Washington 25, D. C.
1	Attn: Dr. G. B. Schubauer, Chief
	Ames Aeronautical Laboratory Moffett Field, California
1	Attn: Walter G. Vincenti
	University of California Observatory 21 Berkeley 4, California
1	Attn: Leland E. Cunningham
	Massachusetts Inst. of Technology Dept. of Mathematics, Room 2-270 77 Massachusetts Avenue Cambridge, Massachusetts
1	Attn: Prof. Eric Reissner
	Graduate School Aeronautical Engr. Cornell University Ithaca, New York
1	Attn: W. R. Sears, Director VIA: CNR
	Applied Math. and Statistics Lab. Stanford University Stanford, California
1	Attn: R. J. Langle, Associate Dir.
	University of Minnesota Dept. of Aeronautical Engr. Minneapolis, Minnesota
1	Attn: Professor R. Hermann

No. of Copies	
	Case Institute of Technology Dept. of Mechanical Engineering Cleveland, Ohio
1	Attn: Professor G. Kuerti VIA: CNR
	Harvard University 109 Pierce Hall Cambridge 38, Massachusetts
1	Attn: Professor R. von Mises

EXTERNAL DISTRIBUTION

No. of Copies	
1	Mr. A. I. Moskovitz Bureau of Ordnance (Re9a) Navy Department Washington, D. C.
1	Chief, Naval Operations Department of the Navy Washington 25, D. C.
2	The Artillery School Anti-aircraft & Guided Missiles Br. Fort Bliss, Texas Attn: Research & Analysis Sec.
1	Dr. K. F. Rubert Internal Aerodynamics Branch National Advisory Committee for Aeronautics Langley Field, Virginia
1	Prof. R. F. Probstein Division of Engineering Brown University Providence, Rhode Island
1	Commander U. S. Naval Proving Ground Dahlgren Virginia
1	Jet Propulsion Laboratory 4800 Oak Grove Drive Pasadena, California Attn: Dr. P. P. Wegener
1	Flight and Aerodynamics Laboratory Research Division Ordnance Missile Laboratory Redstone Arsenal Huntsville, Alabama Attn: J. L. Potter, Chief
5	U. S. Air Force Headquarters Arnold Engineering Development Center (ARDC) Tullahoma, Tennessee Attn: AEKS

No. of Copies	
1	Professor J. Kaye MIT, Physics Department Cambridge, Massachusetts
1	Professor Dean MIT, Gas Turbine Laboratory Engineering Department Cambridge, Massachusetts
1	Dr. Ruldolf Herman Department of Mechanical Engineering University of Minnesota Minneapolis 14, Minnesota
1	Dr. Ernst R. G. Eckert Department of Mechanical Engineering University of Minnesota Minneapolis 14, Minnesota
1	Mr. Mervin Sibulkin Jet Propulsion Laboratory 4800 Oak Grove Drive Pasadena, California
1	Dr. G. R. Eber Holloman Air Force Base Alamagordo, New Mexico
1	Dr. Albert E. Lombard Pentagon, Rm. 4E348 Washington, D. C.
1	Dr A. Ferri Polytechnic Institute of Brooklyn 99 Livingston Street Brooklyn, New York
1	Dr. E. R. Van Driest Aerophysics Laboratory North American Aviation, Inc. Downing, California
1	Dr. Paul A. Libby Polytechnic Institute of Brooklyn 99 Livingston Street Brooklyn, New York
1	Major James B. Robinson, 3rd Air Research & Development Command Washington Air Force Div. Field Office Rm. 4945 Main Navy Bldg. Washington 25, D. C.

No. of Copies	
1	Dr. R. H. Mills Wright Air Development Center Wright-Patterson Air Force Base Dayton, Ohio
3	Mr. Ronald Smelt Chief, Gas Dynamics Facility Arnold Research Organization, Inc. Tullahoma, Tennessee
1	Dr. Henry Nagamatsu California Institute of Technology Pasadena, California
1	Professor N. J. Hoff Polytechnic Institute of Brooklyn Brooklyn, New York
1	Dr. F. L. Wattendorf Facilities Division DCS/Development Hdqts. USAF, Room 5C368 Pentagon, Washington 25, D. C.
1	Professor A. Kantrowitz Cornell University Department of Aeronautical Engineering Ithaca, New York
1	Professor Lester Lees California Institute of Technology Pasadena, California
1	Dr. H. G. Stever MIT, Department of Aeronautical Engineering Cambridge, Massachusetts
1	Professor G. L. Von Eschen Aeronautical Engineering Department Ohio State University Columbus, Ohio
1	Mr. R. L. Bayless Consolidated Vultee Aircraft Corporation San Diego, California
1	Professor S. M. Bogdonoff Department of Aeronautical Engineering Princeton University Princeton, New Jersey